TABLE OF CONTENTS

LIST OF TABLES

LIST OF FIGURES

3.2.S.3.1. ELUCIDATION OF STRUCTURE AND OTHER CHARACTERISTICS

3.2.S.3.1.1. Introduction

This section describes the structure and characteristics of BNT162b2 drug substance (DS) which have been assessed using the analytical approaches outlined in Table 3.2.S.3.1-1. The analytical methodologies employed for BNT162b2 RNA drug substance characterization are capable of evaluating primary structure, including 5'-capping and 3'-poly(A) tail, and higher order structure. The results demonstrate that BNT162b2 RNA drug substance has the expected structure.

Analytical characterization was performed with BNT162b2 drug substance batch (20Y513C101), which is representative of the commercial process.

Table 3.2.S.3.1-1. Characterization Strategy for BNT162B2 Drug Substance

Characteristic	Analytical Approach	Methodology	Section References
Primary structure	Confirm expected RNA sequence at the oligonucleotide level	Reversed phase HPLC-UV and tandem mass spectrometry (LC/MS/MS) – of oligonucleotide fragments generated by RNAse T1 digestion	Section 3.2.S.3.1.2.1
	Confirm expected RNA sequence at the oligonucleotide level	[redacted] Next Generation Sequencing Technology	Section 3.2.S.3.1.2.2
5'-Cap structure	Confirm the 5' capping structure and 5'-end profile	Reversed phase HPLC-UV and mass spectrometry (LC-UV/MS) analysis of purified 5′ terminal after RNaseH digestion	Section 3.2.S.3.1.3
Poly(A)-tail	Confirm the presence and determine the length of poly(A)-tail	Reversed phase HPLC-UV and mass spectrometry (LC-UV/MS) analysis of purified poly(A)-tail after Ribonuclease T1 digestion	Section 3.2.S.3.1.4
Higher order structure (HOS)	Spectroscopic analysis to confirm the presence and fingerprint of HOS	Circular dichroism (CD) spectroscopy	Section 3.2.S.3.1.5
Biological Activity	Confirm size of expressed protein Confirm spike protein expression	Western analysis Cell-based flow cytometry	Section 3.2.S.3.1.6

3.2.S.3.1.2. Primary Structure

3.2.S.3.1.2.1. LC/MS/MS - Oligonucleotide Mapping

The primary sequence of BNT162b2 DS was analyzed by LC/MS/MS - oligonucleotide mapping. BNT162b2 DS was digested with RNAse T1, and the resulting enzymatic fragments were separated by ion-paired reversed-phase high performance liquid chromatography (IP-RP-HPLC) with UV detection at [redacted] (Figure 3.2.S.3.1-1 through Figure 3.2.S.3.1-5). [redacted]

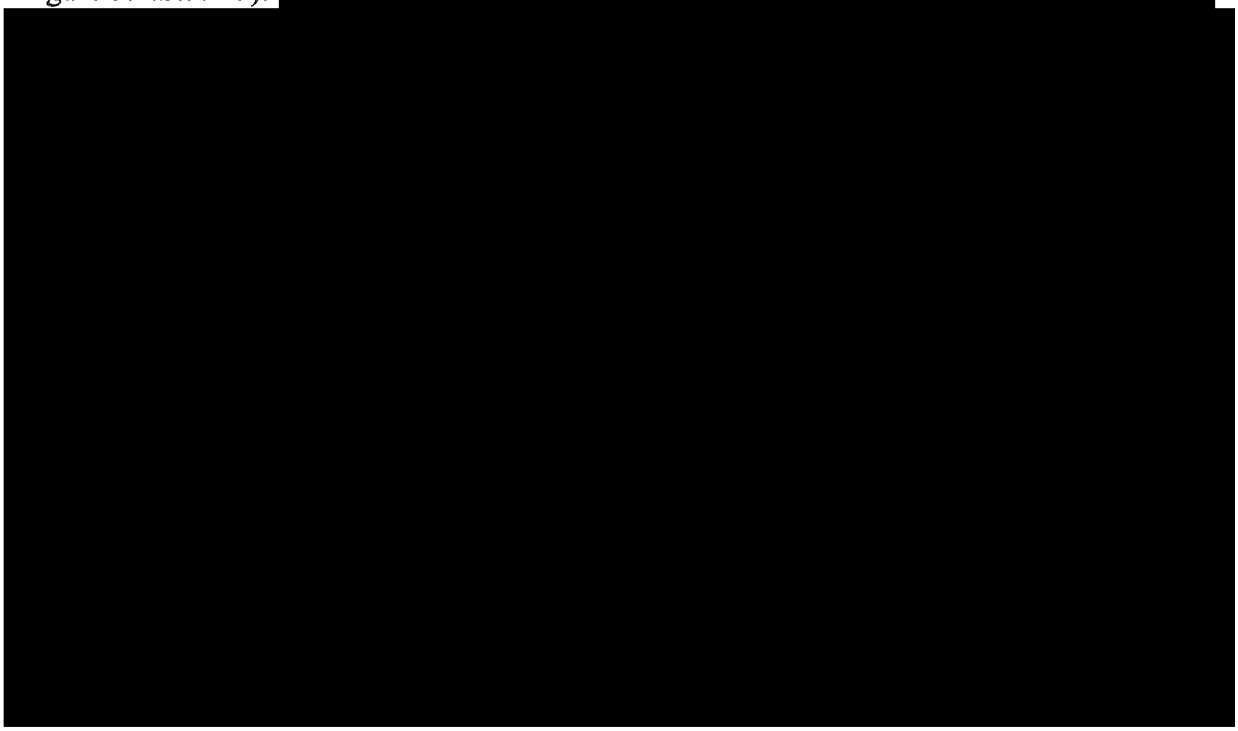

The LC/MS/MS – oligonucleotide mapping results are summarized in Table 3.2.S.3.1-3 and demonstrate that BNT162b2 DS contains the correct sequence as predicted from the linear DNA template (Section 3.2.S.2.3 Source, History and Generation of Plasmids).

Figure 3.2.S.3.1-1. LC/MS/MS – Oligonucleotide Mapping of BNT162b2 DS ([redacted]

Figure 3.2.S.3.1-2. LC/MS/MS – Oligonucleotide Mapping of BNT162b2 DS [redacted]

Figure 3.2.S.3.1-3. LC/MS/MS – Oligonucleotide Mapping of BNT162b2 DS [redacted]

Figure 3.2.S.3.1-4. LC/MS/MS – Oligonucleotide Mapping of BNT162b2 DS [redacted]

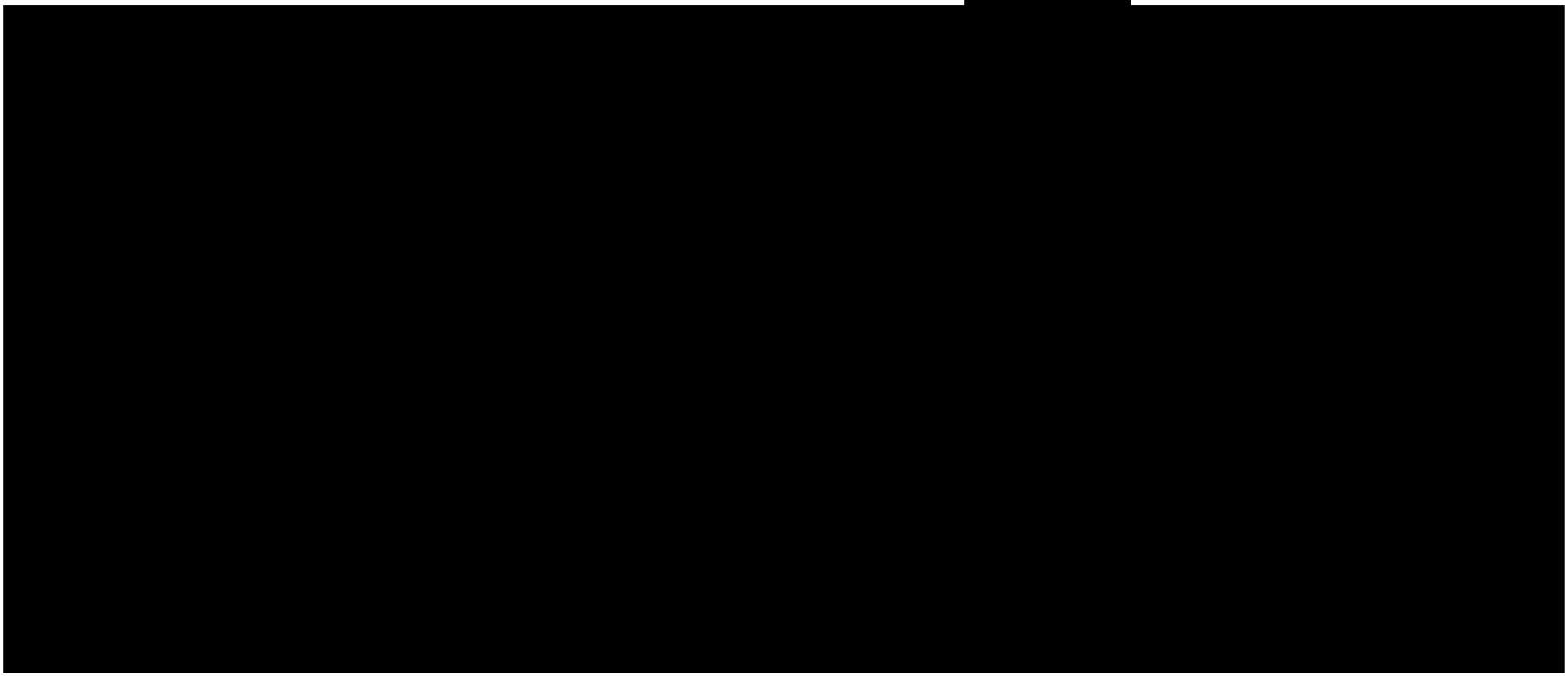

Figure 3.2.S.3.1-5. LC/MS/MS – Oligonucleotide Mapping of BNT162b2 DS [redacted]

Table 3.2.S.3.1-2. LC-MS/MS – Oligonucleotide Mapping Sequence Coverage for BNT162b2

[redacted]

Table 3.2.S.3.1-3. LC/MS/MS – Oligonucleotide Mapping Summary of BNT162b2 DS

Characteristics	Results
RNA sequence confirmation	BNT162b2 DS sequence coverage: Detected nucleotides represent [redacted] (Table 3.2.S.3.1-2)
RNA termini	[redacted] - oligonucleotide mapping – see 3.2.S.3.1.3 for detailed analysis of 5' terminus [redacted] (see 3.2.S.3.1.4 for detailed analysis of PolyA tail)

3.2.S.3.1.2.2. Sequencing of RNA

In order to further confirm sequence identity, RNA sequencing for BNT162b2 DS was performed using the [redacted]

[redacted]

Taken together, the RNA sequencing results further demonstrate that the BNT162b2 transcript generated during the *in vitro* transcription (IVT) process bears the correct RNA sequence as predicted from the linear DNA template (Section 3.2.S.2.3 Source, History and Generation of Plasmids).

Figure 3.2.S.3.1-6. BNT162b2 mRNA: RNAseq Coverage Plot

3.2.S.3.1.3. 5'-Cap Characterization by LC-UV/MS

The characterization of the 5' end capped (5'-Cap) and un-capped species of BNT162b2 DS was accomplished by ion-pair reversed-phase high performance liquid chromatography-ultraviolet light detection at [redacted] and online electrospray ionization mass spectrometry (RP-HPLC/UV-ESI MS) or LC-UV/MS. Sample handling and chromatography follow the method described in Section 3.2.S.4.2 Reversed Phase – High Performance Liquid Chromatography (RP-HPLC). Briefly, the target RNA was annealed to a biotinylated probe designed to complement to the last 26 bases of its 5' end, then treated with RNase H to cleave the annealed 5' end from the much larger mRNA remnant. The duplex was affinity-purified using streptavidin-coated magnetic beads. The short 5' oligonucleotide capped and un-capped RNase cleaved fragments were eluted from the beads and the eluant analyzed by RP-HPLC/UV-ESI MS. In general, the ion-pair RP-HPLC-UV method separates species by the number of nucleotide residues, with shorter oligonucleotides eluting before longer oligonucleotides.

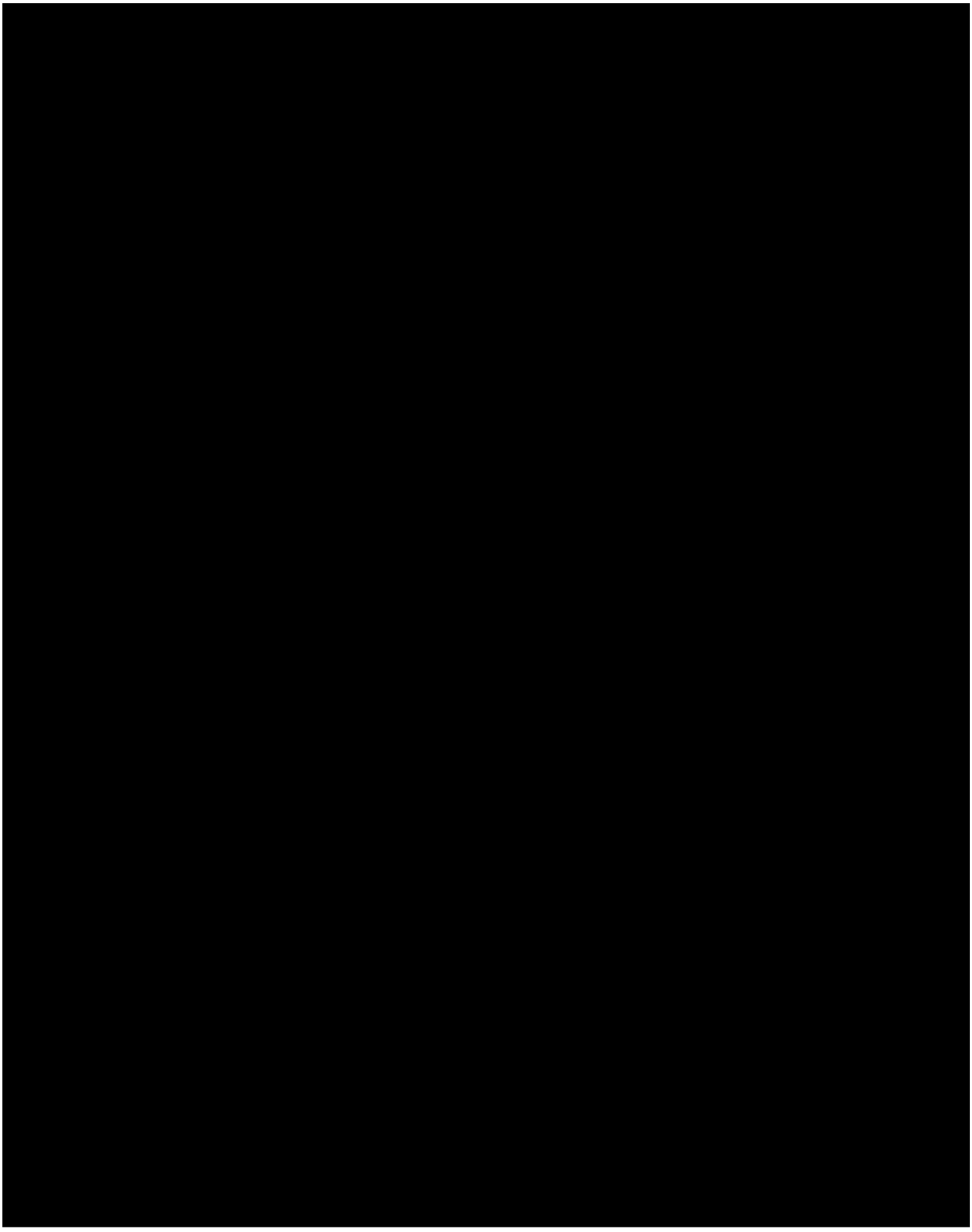

Figure 3.2.S.3.1-7. 5'-Cap Assay UV Chromatogram of BNT162b2 DS

Figure 3.2.S.3.1-8. Mass Spectra of 5'-Cap, 5'-ppp and 5'-pp RNase Cleaved Fragments from BNT162b2 DS

Table 3.2.S.3.1-4. Accurate Mass Assignments for BNT162b2 DS 5′-Cap and non-Cap RNase Cleaved Fragments

[redacted]

3.2.S.3.1.4. 3′ Poly(A)-tail Characterization by LC-UV/MS

Analysis of the 3′ polyadenosine tail (poly(A)-tail) of BNT162b2 DS was accomplished by ion-pair reversed-phase high performance liquid chromatography with UV detection at [redacted] and on-line electrospray ionization mass spectrometry (RP-HPLC-UV/ESI MS or LC-UV/MS). The poly(A)-tail of BNT162b2 DS was cleaved off by ribonuclease T1 (RNase T1) followed by isolation via [redacted] affinity purification.

[redacted]

Figure 3.2.S.3.1-9. RP-HPLC-UV Profile [redacted] of Extracted BNT162b2 DS Poly(A)-tail

Figure 3.2.S.3.1-10. Mass Spectrum of A30 Poly(A) Segment

Figure 3.2.S.3.1-11. Mass Spectrum of L70 Poly(A) Segment

Table 3.2.S.3.1-5. Accurate Mass Assignments for BNT162b2 DS Poly(A)-tail

Poly(A) Segment	Sequence[a]	Number of Adenosines Observed (n)	Theoretical Masses (Da)[b]	Observed Masses (Da)[c]	Relative Abundance[d]
[redacted]					

3.2.S.3.1.5. Higher Order Structure

The higher order structure of BNT162b2 mRNA DS was characterized in solution using [redacted]

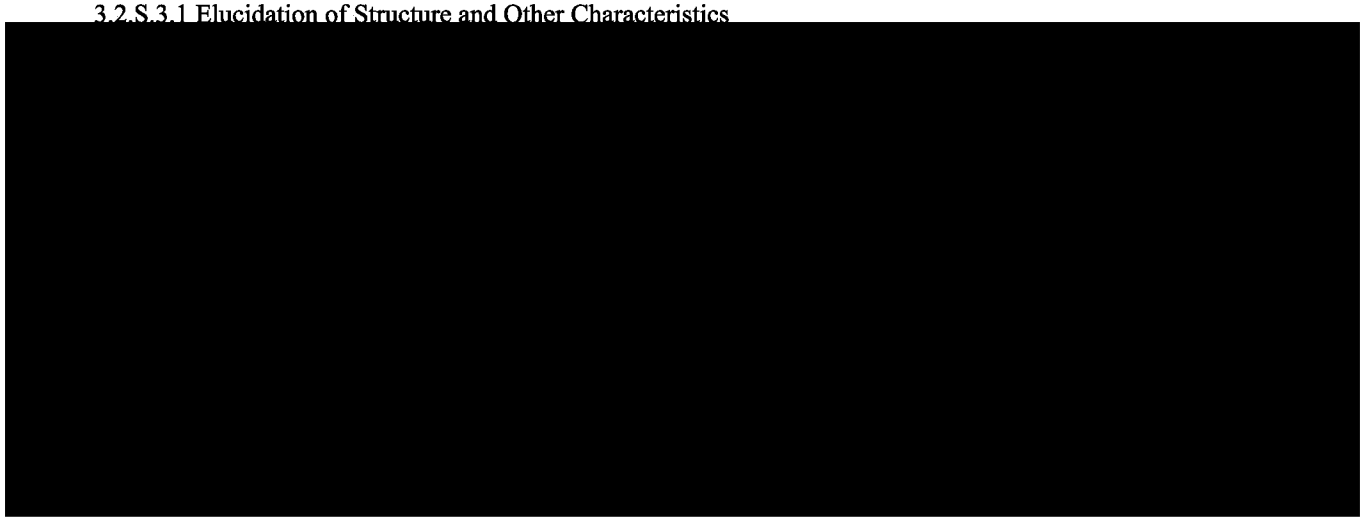

Figure 3.2.S.3.1-12 CD spectrum of BNT162b2 mRNA

[redacted]

3.2.S.3.1.6. Biological Activity of BNT162b2 DS

The BNT162b2 RNA DS is formulated in lipid nanoparticles to create the drug product (DP). The lipid nanoparticle DP enables delivery of the RNA into host cells to allow expression of the SARS-CoV-2 S antigen and develop immune response. To characterize the biological activity of BNT162b2 RNA DS, a Western blot was used to evaluate the size of the expressed protein through transfection into [redacted] In addition, a cell-based flow cytometry method was used to enumerate the population of cells which express the SARS-CoV-2 antigen encoded by the RNA in a DP sample.

3.2.S.3.1.6.1. Expressed protein size by Western blot

[redacted]

Figure 3.2.S.3.1-13. BNT162b2 Expressed Protein Size by Western Blot

[redacted]

Table 3.2.S.3.1-6. Theoretical protein size after BNT162b2 expression

	S Protein with Signal Peptide	Mature S Protein	S1 Subdomain	S2 Subdomain
Residues	1-1273	13-1273	13-685	686-1273
# Amino Acids	1273	1261	673	588
Aglycosylated MW [Da]	141115.0	139755.3	75310.7	64462.6
Glycosylated MW[a] [Da]	192862.6	191502.9	105888.8	85632.0

Theoretical masses assume full occupancy of all 22 N-linked glycosylation sites with sialylated G2F+2NeuAc.

Additionally, an enzymatic deglycosylation of the expressed proteins following BNT162b2 transfection into HEK-293 was pursued. In this study, increasing volumes of the de-glycosylating enzyme PNGase F were added to transfected cell lysates, and the resulting samples were analyzed by Western blot, with detection using antibodies specific for the S1 domain, the receptor binding domain (RBD, located within the S1 domain), and the S2 domain. The resulting Western blot is shown in Figure 3.2.S.3.1-14. Upon PNGase F digestion, new bands ranging from ~40 kDa to ~140 kDa are detected. The ~140 kDa protein detected by the anti-Spike protein S1 domain antibody, anti-spike protein S2 domain antibody and anti-spike protein S1 domain RBD antibody is consistent with the deglycosylated full-length spike protein (S1S2). The band of ~75 kDa detected by anti-Spike protein S1 domain antibody and anti-spike protein S1 domain RBD antibody is consistent with deglycosylated S1 domain. The band of ~64 kDa detected only by anti-Spike protein S2 domain antibody is consistent with deglycosylated S2 domain. The new ~40kDa band detected by the anti-S1 and anti-RBD antibodies and the new band of ~90 kDa detected by anti-S2 antibody are believed to be the result of further proteolysis of the S1S2 spike protein within the cell lysate during PNGase F treatment steps. High molecular weight bands in the Western blot (i.e. > 230 kDa) likely result from aggregated spike proteins that are not fully denatured during sample preparation.

Figure 3.2.S.3.1-14. Deglycosylated proteins after BNT162b2 transfection are consistent with the S1S2 protein

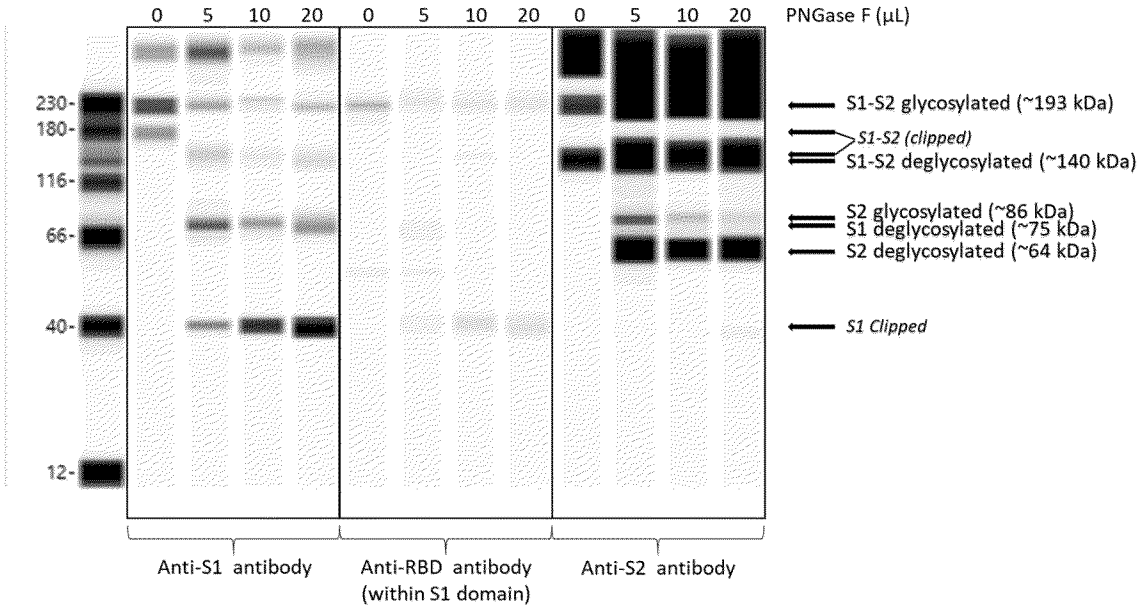

3.2.S.3.1.6.2. In Vitro Expression by Cell-Based Flow Cytometry

The in vitro expression of SARS-CoV-2 spike protein encoded by the RNA in BNT162b2 DS batch 20Y513C101, which has been formulated into lipid nanoparticle drug product (DP) was determined. DS batch 20Y513C101 was used in the production of DP lots EE8492 and EE8493. This analysis was performed using the method described in Section 3.2.P.5.2 Analytical Procedures – Cell-based Flow Cytometry.

Human embryonic kidney (HEK293T) cells were transfected with BNT162b2 DP. After incubation, the cells were harvested and transferred to assay plates. Transfected cells were stained, fixed, and permeabilized. Fixative was washed from the cells and a SARS-CoV-2 spike S1 primary antibody was added, which binds to any surface-expressed and intracellular SARS-CoV-2 S1 antigen. [redacted] Cells were analyzed by flow cytometry where the in vitro expression of the SARS-CoV-2 spike was determined as the percent positive cells (S1+) from the viable, single cell population. The results of this analysis are provided in Table 3.2.S.3.1-7.

Table 3.2.S.3.1-7. In Vitro Expression of BNT162b2 Drug Product

Drug Product Lot	Drug Substance Batch	In Vitro Expression (% positive cells)
EE8492	20Y513C101	[redacted]
EE8493	20Y513C101	

3.2.S.3.1.7. Heightened Characterization of BNT162b2 Fragment Species

The BNT162b2 fragment profile is measured using the Fragment Analyzer CGE method, which enables quantitation of RNA integrity (intact RNA content). It is expected that a majority of the fragmented species are generated by premature transcriptional stops or mRNA hydrolysis. In the study described below, the fragmented species were evaluated for the presence of 5'-cap and poly(A) tail elements needed for protein expression, and the potential for fragment species to express truncated or off-target protein antigens was evalutated.

Additional characterization of intact and fragment species isolated using ion pairing (IP) RP-HPLC

DS batch R427-P020.2-DS (Process 1) and batch 20Y513C501 (Process 2) samples were fractionated using ion pairing RP-HPLC to further characterize the drug substance mRNA species. The samples of the active substance are representative of the finished product, as the fragment species profile is consistent between DS and DP, with only minor increases to the fragment content during DP manufacturing.

Figure 3.2.S.3.1-15 shows the ion pairing RP-HPLC chromatograms for batches R427-P020.2-DS and 20Y513C501. For both batches, two peaks are observed by IP-RP-HPLC. Fragment Analyzer electropherograms (Figure 3.2.S.3.1-16) demonstrate that Peak 1 consists almost entirely of fragmented species. The Peak 2 electropherogram demonstrates that the predominant species is consistent with the main peak observed by fragment analyzer, with lower levels of fragments compared with the starting material.

Figure 3.2.S.3.1-15. Ion Pairing RP-HPLC Chromatograms for DS batches R427-P020.2-DS and 20Y513C501

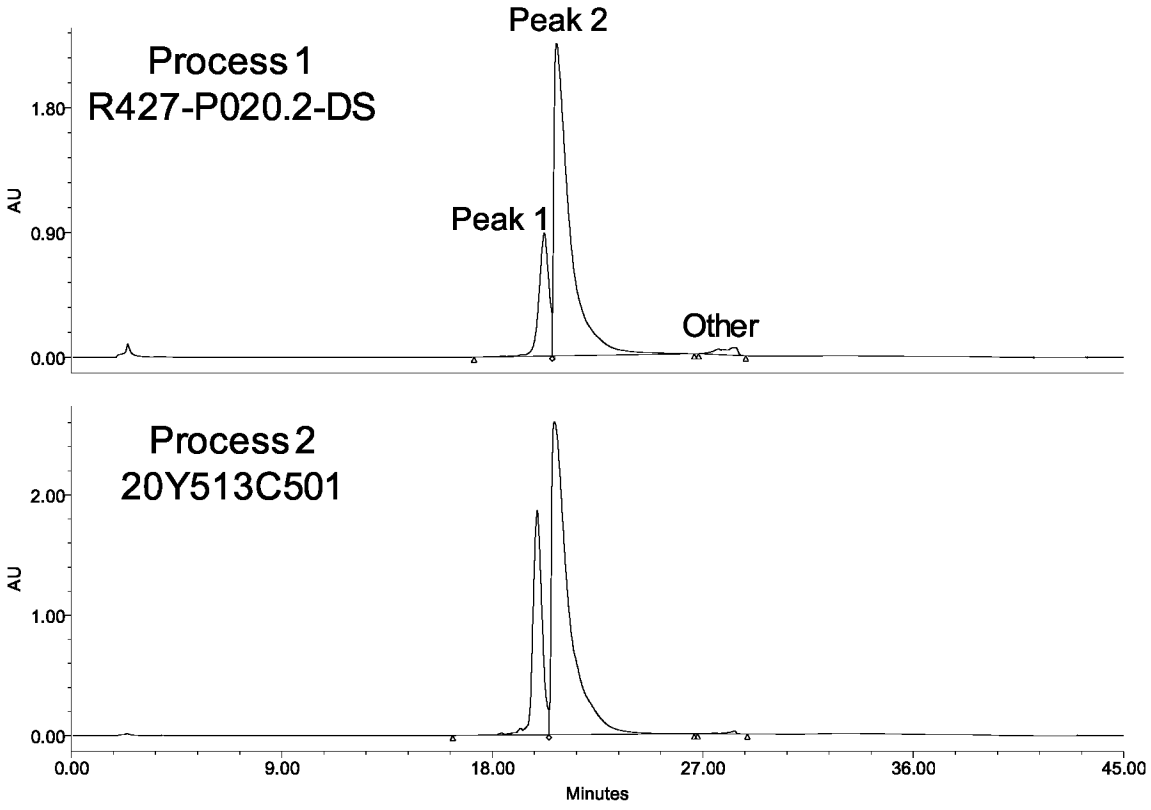

Figure 3.2.S.3.1-16. Fragment Analyzer Electropherograms of Peak 1, Peak 2, and Unfractionated DS

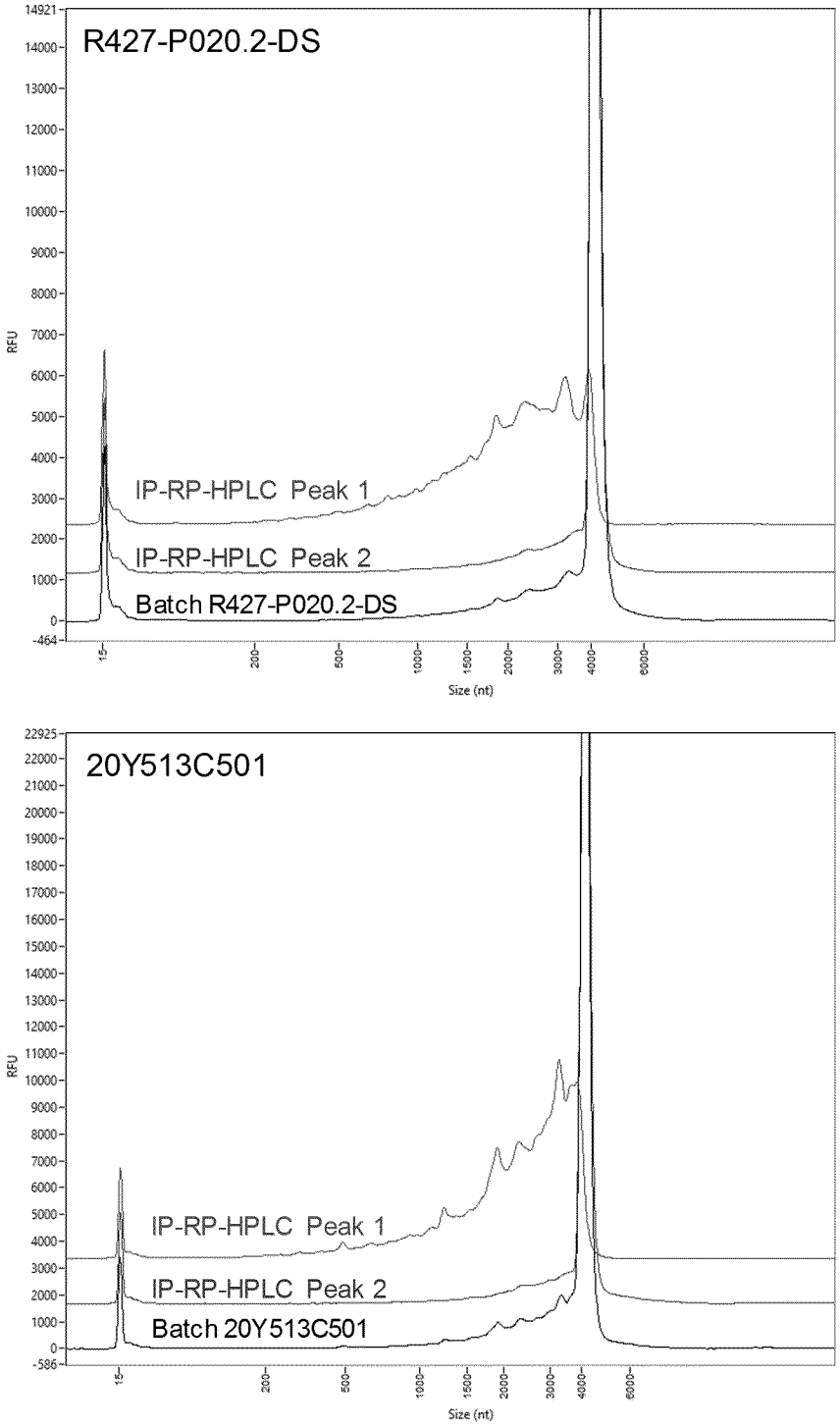

Peaks 1 and 2 from each DS batch (R427-P020.2-DS and 20Y513C501) were then isolated and characterized to compare 5'-cap and poly(A) tail length to that of unfractionated material. Table 3.2.S.3.1-8 shows that 5'-cap and non-cap species content is unchanged across Peak 1, Peak 2, and unfractionated starting materials, consistent with previous characterization data. Additionally, comparable 5'-cap chromatographic profiles were observed for all six samples (Figure 3.2.S.3.1-17).

Table 3.2.S.3.1-8. 5'-Cap Species Content

Sample	Early Non-Cap (%)	5'-Cap (%)	Late Non-Cap (%)
R427-P020.2-DS			
Peak 1 (R427-P020.2-DS)			
Peak 2 (R427-P020.2-DS)			
20Y513C501			
Peak 1 (20Y513C501)			
Peak 2 (20Y513C501)			

Figure 3.2.S.3.1-17. 5'-Cap Chromatograms of BNT162b2 DS, Peak 1, and Peak 2 Samples

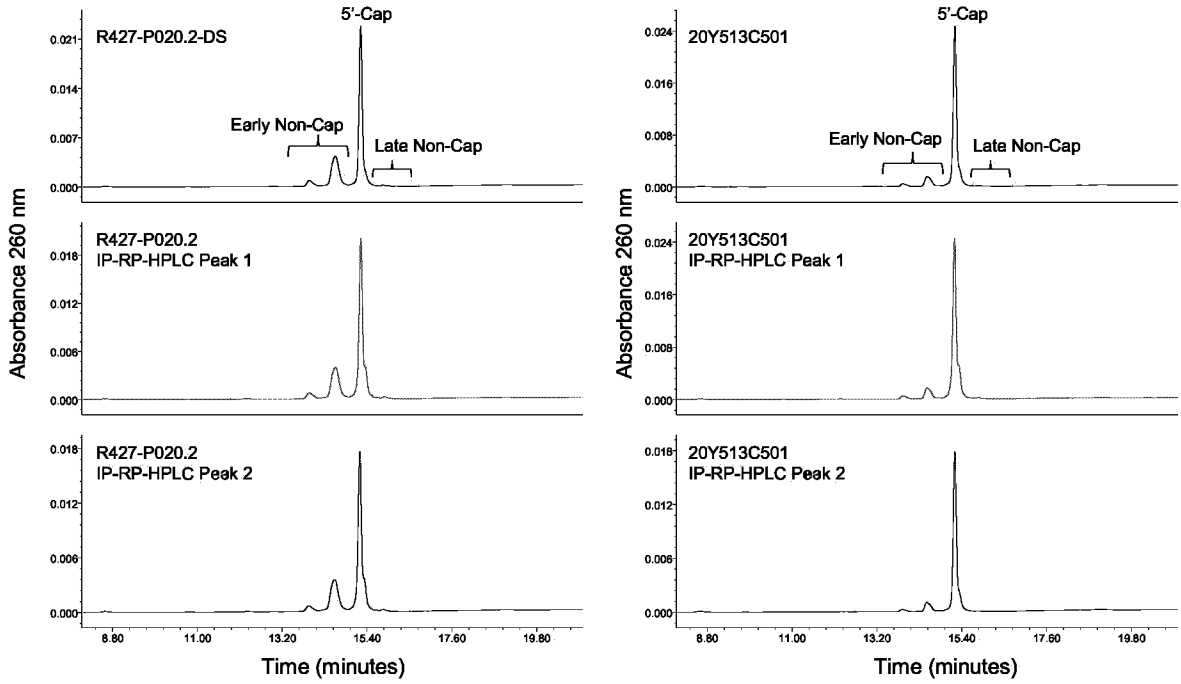

In contrast to 5'-cap, characterization of the poly(A) tail length and distribution by IP-RP-HPLC demonstrates that the fragment species in Peak 1 lack poly(A) tail, while the Peak 2 and unfractionated starting DS samples show the expected length and distribution for the BNT162b2 poly(A) tail (Figure 3.2.S.3.1-18). These results support the conclusion that a significant proportion of fragment species in BNT162b2 are 5'-capped at levels consistent

with the intact transcript, but predominantly lack the poly(A) tail, likely arising from premature transcriptional stops during production.

Quantitation of the poly(A) tail content by ddPCR further confirms that the fragment species in Peak 1 lack significant poly(A) tail content (< LOQ), while the Peak 2 and starting DS materials for both R427-P020.2-DS and 20Y513C501 contain [redacted] poly(A) tail content (Table 3.2.S.3.1-9). Additionally, the poly(A) tail content in Peak 2 fractions is consistently higher than the starting material, indicating enrichment of intact (i.e. poly-adenylated) transcripts in these samples.

Table 3.2.S.3.1-9. Poly(A) Tail Content

Sample	Poly(A) Tail Content (%)
R427-P020.2-DS	[redacted]
Peak 1 (R427-P020.2-DS)	
Peak 2 (R427-P020.2-DS)	
20Y513C501	
Peak 1 (20Y513C501)	
Peak 2 (20Y513C501)	

LOQ = Limit of Quantitation

Figure 3.2.S.3.1-18. Poly(A) Length and Distribution of BNT162b2 DS, Peak 1, and Peak 2 Samples

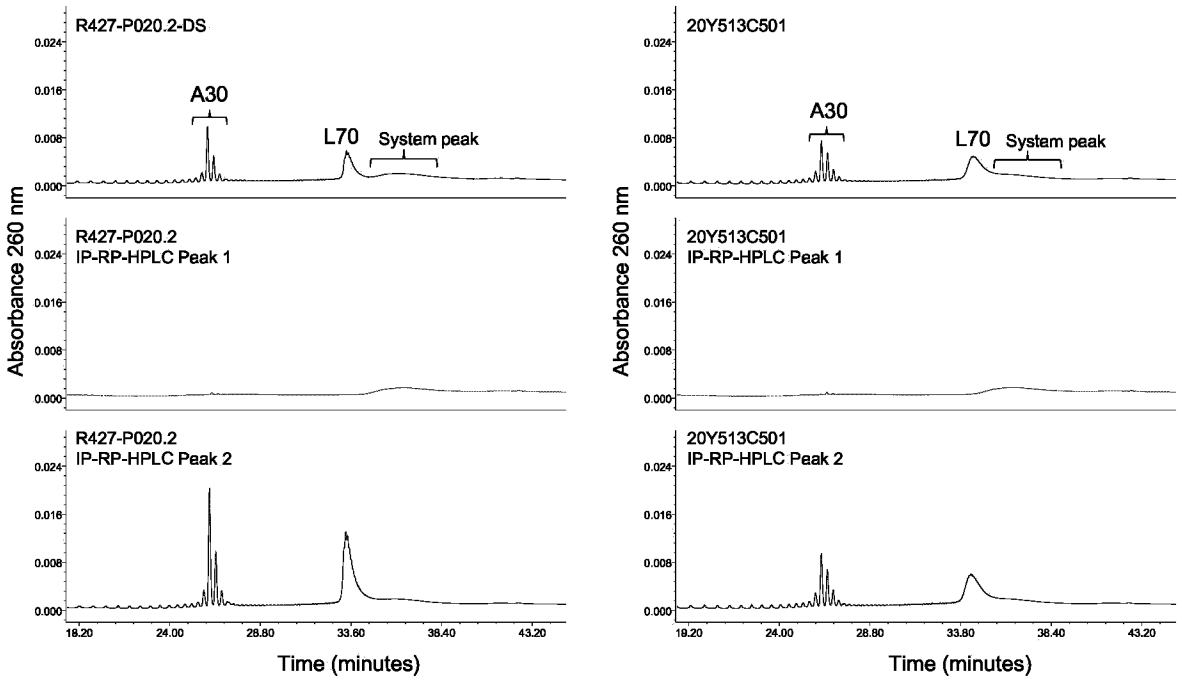

Assessment of the potential for translation into truncated S1S2 or other off-target proteins/peptides

To assess the potential for translation of mRNA fragments into truncated S1S2 proteins/peptides or other proteins/peptides, two orthogonal protein expression systems were utilized and translated proteins were evaluated by Western blot.

As shown in Section 3.2.S.2.6 Development History and Comparability Assessment and Section 3.2.S.3.1.6.1, Western blot of BNT162b2-transfected cell lysates demonstrates expression of the S1S2 protein antigen. In addition, truncated protein species were not observed by Western blot in DS batches that contained up to 40% fragment species.

To test the hypothesis that transcripts require both 5'-cap and poly(A) to support protein translation, full-length transcripts lacking either 5'-cap or poly(A) tail were transfected into HEK-293 cells, and the resulting cell lysates were analyzed by Western blot using detection antibodies specific for the S1 or S2 domain. In contrast to BNT162b2 DS, which shows the expected banding pattern for the S1S2 protein antigen, S1S2 protein bands were not detected for the transcripts lacking either the 5'-cap (Figure 3.2.S.3.1-19) or the poly(A) tail (Figure 3.2.S.3.1-20). This control experiment using full-length transcripts demonstrates that both 5'-cap and poly(A) tail are required for protein expression.

Figure 3.2.S.3.1-19. Full-Length Transcripts Require 5'-Cap for Translation

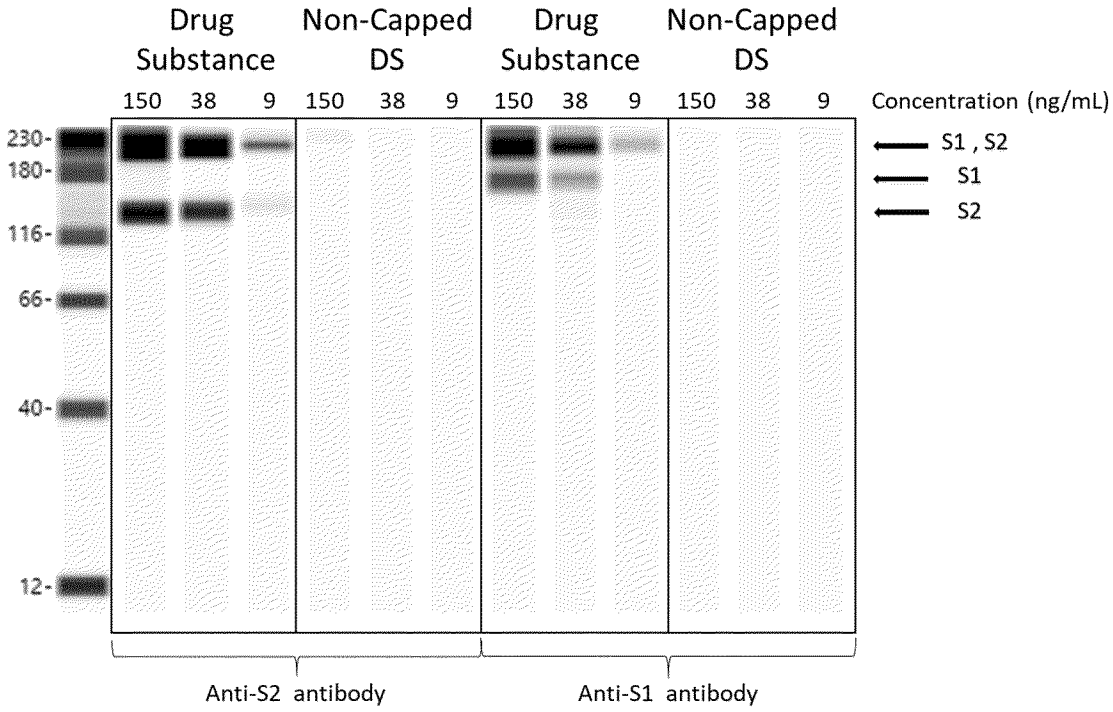

Figure 3.2.S.3.1-20. Full-Length Transcripts Require Poly(A) Tail for Expression

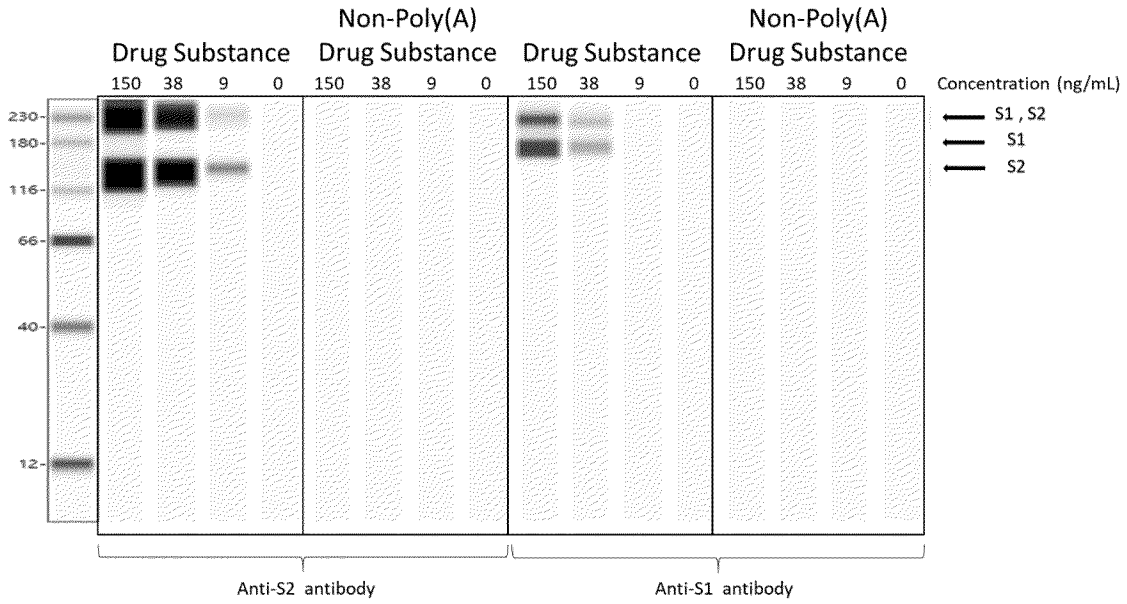

Consistent with the results using full-length mRNA transcripts, cells transfected with the starting DS batches (R427-P020.2-DS and 20Y513C501) or with Peak 2 material (isolated using IP-RP-HPLC above) show comparable spike protein expression by Western blot, whereas cells transfected with the Peak 1 material comprised of fragmented species do not show evidence of protein expression (Figure 3.2.S.3.1-21). The results are consistent for both Process 1 and Process 2 batches, and both show a dose-dependent expression response for the unfractionated DS and Peak 2 samples.

Figure 3.2.S.3.1-21. Western Blot of Peak 1, Peak 2, and Starting DS Material

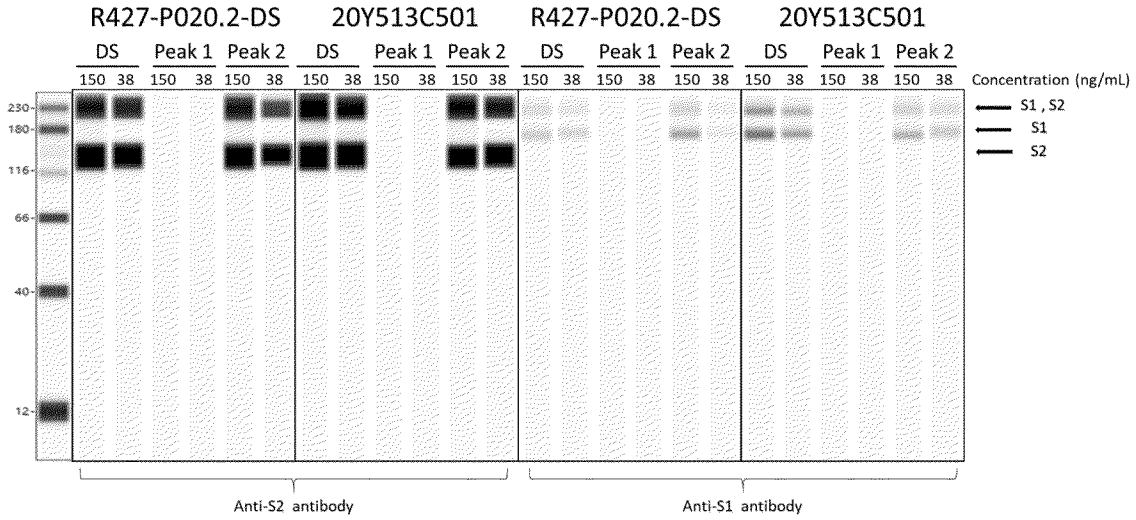

In a separate experiment, the potential for truncated transcripts to produce protein/peptides was evaluating using a cell-free in vitro expression system. The cell-free in vitro translation is performed using the commercially available Rabbit Reticulocyte Lysate (RRL) system, which is provided by Promega. The key components for the in vitro translation reaction are the RRL, the amino acid mixtures as well as a precharged, biotin-labeled, lysine tRNA. During the translation reaction the labeled lysines are incorporated into the nascent protein chain, which enables the visualization of the resulting protein. For that, after completion of the translation reaction, the samples are subjected to a denaturing gel electrophoresis procedure (SDS-PAGE; Sodium Dodecyl Sulfate Polyacrylamide Gel Electrophoresis) followed by the transfer to a nitrocellulose membrane via electroblotting. The visualization of the protein is achieved by binding of the biotin-labeled lysines to Streptavidin-Alkaline Phosphatase (Strep-AP) followed by colorimetric detection.

As a positive control, a luciferase-encoding RNA is used, which is provided within the translation kit and results in a protein band at a size of approximately 60 kDa. A negative control sample was generated, which was subjected the complete assay workflow without any RNA in the reaction mixture to determine background signals that are not related to the RNA of the test sample.

The RNA that was used in the in vitro translation study was produced as engineering run in the BioNTech Mainz / Rentschler manufacturing node generating representative material according to the commercial process (batch no: 1071509; 37.6 L IVT reaction; 180 L drug substance; expected protein size: approx. 140 kDa). The batch data are presented in

Table 3.2.S.3.1-10. Batch data of the engineering run 1071509 (BioNTech Mainz/ Rentschler)

Parameter	Result
RNA integrity	[redacted]
dsRNA	[redacted]pg dsRNA / µg RNA
Residual DNA template	[redacted]ng DNA / mg RNA
Identity of encoded RNA sequence	Identity confirmed
Appearance (Coloration)	Not more intensely colored than level 7 of brown (B) color standard
Appearance (Clarity)	[redacted]NTU
Content (RNA concentration)	[redacted]mg/mL
Bioburden	0 CFU / 10 mL
Endotoxins	< 1.0 EU/mL
pH	[redacted]
5′-Cap	[redacted]
Poly(A) tail	[redacted]

BNT162b2 Process 2 batch 1071509 was intentionally degraded by exposure to elevated temperature, generating samples with various levels of fragmented species (Table 3.2.S.3.1-11). Fragment species in thermally degraded samples are generated by hydrolysis, which is the expected degradation pathway subsequent to in-vitro transcription

(i.e. in the DP manufacturing process). The starting and degraded materials were subjected to in vitro expression using rabbit reticulocyte lysate, wherein biotinylated lysine is incorporated into newly translated proteins and peptides for detection by Western blot. This approach enables detection of both truncated S1S2 or other proteins/peptides, if present, without the need for protein/peptide-specific detection antibodies. After in vitro expression, the non-degraded BNT162b2 sample produced a protein approximately 140 kDa, which is consistent with the expected size of the aglycosylated S1S2 protein (denoted with a "*" in Figure 3.2.S.3.1-22). In this cell-free expression system, which lacks the cellular components required for glycosylation, the BNT162b2 expression indicates that a single, full-length or mature S1S2 protein of approximately 140 kDa is produced. For degraded samples, RNA integrity correlated with Western blot band intensity for the full-length protein; however, no truncated or other protein species were detected beyond the background bands observed in the negative control sample (NC).

Table 3.2.S.3.1-11. Thermally Degraded BNT162b2 Drug Substance

Sample	Degradation Time (min)	RNA Integrity (%)
1071509	0	[redacted]
1071509-2	2	
1071509-4	4	
1071509-6	6	
1071509-9	9	
1071509-10	10	
1071509-20	20	

Figure 3.2.S.3.1-22. In vitro translation of degraded BNT162b2 by Western blot

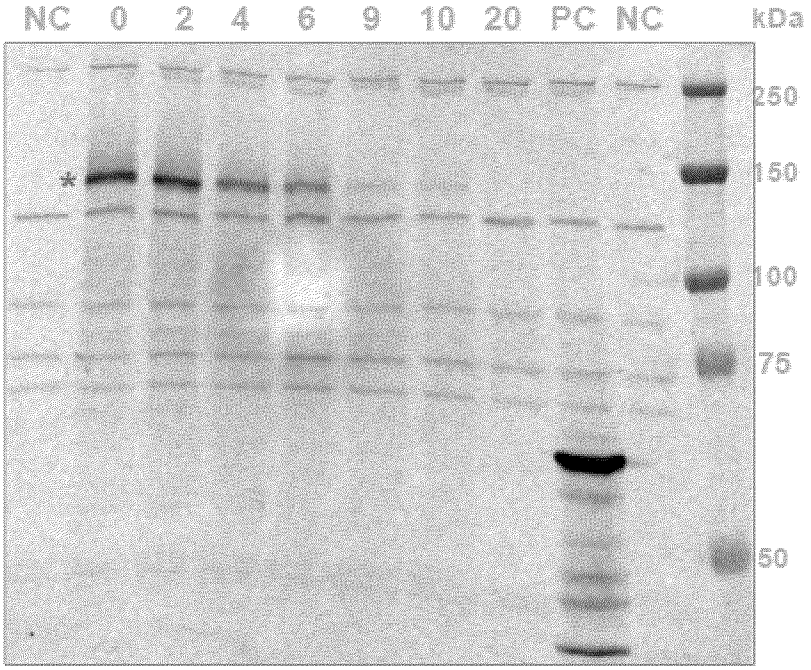

The additional characterization data support the following conclusions:

- Fragment species observed by Fragment Analyzer are consistent across DS Process 1 and Process 2
  - Fragment species isolated using IP-RP-HPLC (Peak 1) contain 5'-cap, but lack poly(A) tail
  - IP-RP-HPLC Peak 2, which is predominantly comprised of intact RNA, include 5'-capped and poly-adenylated species
- 5'-cap and poly(A) tail are required for translation of the full-length BNT162b2 transcript
- Evaluation of full-length and degraded/fragmented transcript expression in two orthogonal expression systems shows no evidence of truncated S1S2 or other proteins or peptides

Taken together, the characterization studies support the assessment that the BNT162b2 fragment species do not pose a risk of mRNA translation resulting in off-target proteins or peptides.

Literature References:

Benjamin D, Sato T, Cibulskis K, et al. Calling Somatic SNVs and Indels with Mutect2. bioRxiv 2019; 10.1101/861054.

Beverly M, Hagen C, Slack O. Poly A tail length analysis of in vitro transcribed mRNA by LC-MS. Anal. Bioanal. Chem. 2018; 410:1667-1677

Clopper C J, and Pearson E S. The Use of Confidence or Fiducial Limits Illustrated in the Case of the Binomial. Biometrika 1934; 26:404–413.

Poplin R, Ruano-Rubio V, DePristo M A, et al. Scaling accurate genetic variant discovery to tens of thousands of samples. bioRxiv 2018; 10.1101/201178.